Talk 2: Boulder Summer School, July 2016

Dirac and Weyl Semimetals and the chiral anomaly

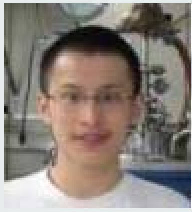
Jun Xiong


Kushwaha


Tian Liang


Jason Krizan


Hirschberger


Zhijun Wang

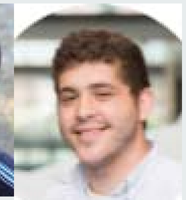
Quinn Gibson


Cano


Bradlyn


Jinwoong Kim

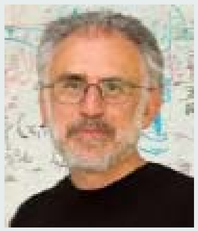
Kioussis

Cal State Northridge

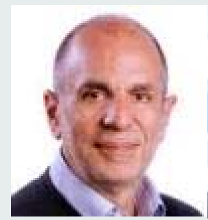
Bob Cava


Bernevig


NPO

Princeton University

1. Chiral anomaly in the half-Heusler GdPtBi
2. Thermopower of Weyl fermions
3. Gap closing in a semiconductor– route to Weyl nodes
4. Topological metal in PbSnTe with large Berry curvature

Support from
Moore Foundation, ARO, NSF

Creation of Weyl states in applied magnetic field

B field

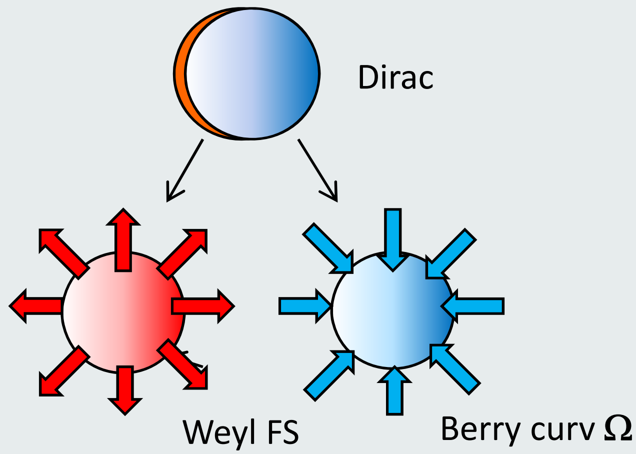

$$\chi = \frac{1}{2\pi} \oint \mathbf{\Omega} \cdot \mathbf{dS}(\mathbf{k})$$

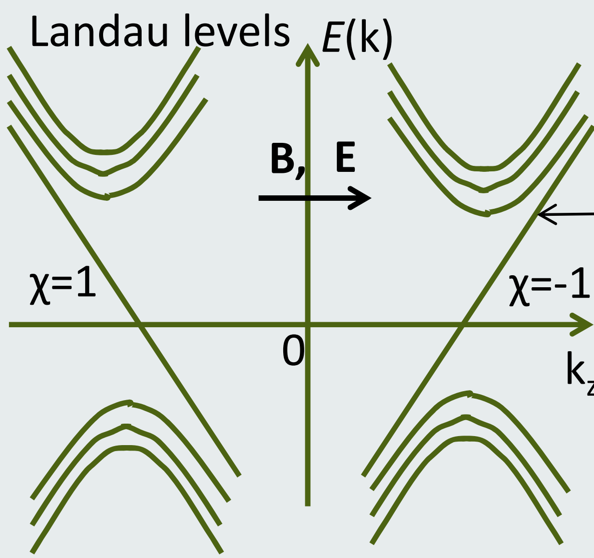

Lowest Landau level
Schwinger model

Detect axial current

1. **Chiral anomaly in a half Heusler GdPtBi**
2. Thermopower of Weyl fermions
3. Gap closing in a semiconductor– route to Weyl nodes
4. Topological metal in PbSnTe with large Berry curvature

Non-metallic Crystals of Na_3Bi with lower carrier density

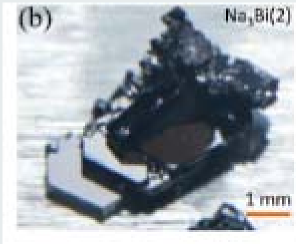

Jun Xiong, S. Kushwaha et al., Science 2015

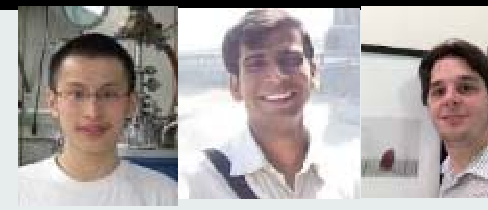

Jun Xiong, S. Kushwaha, Krizan,

Long-term annealed crystals with E_F much closer to node

$$A = -V \frac{e^3}{4\pi^2\hbar^2} \mathbf{E} . \mathbf{B}$$

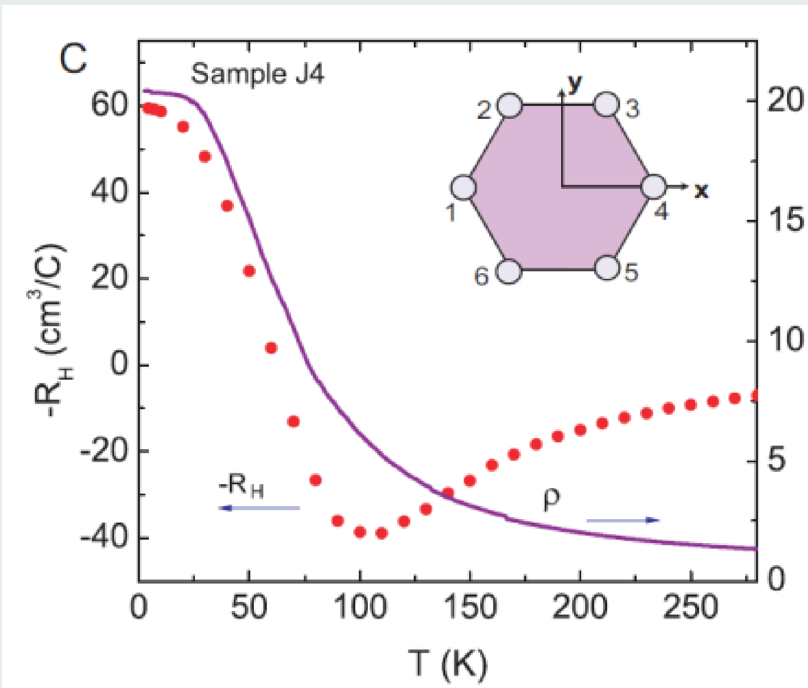

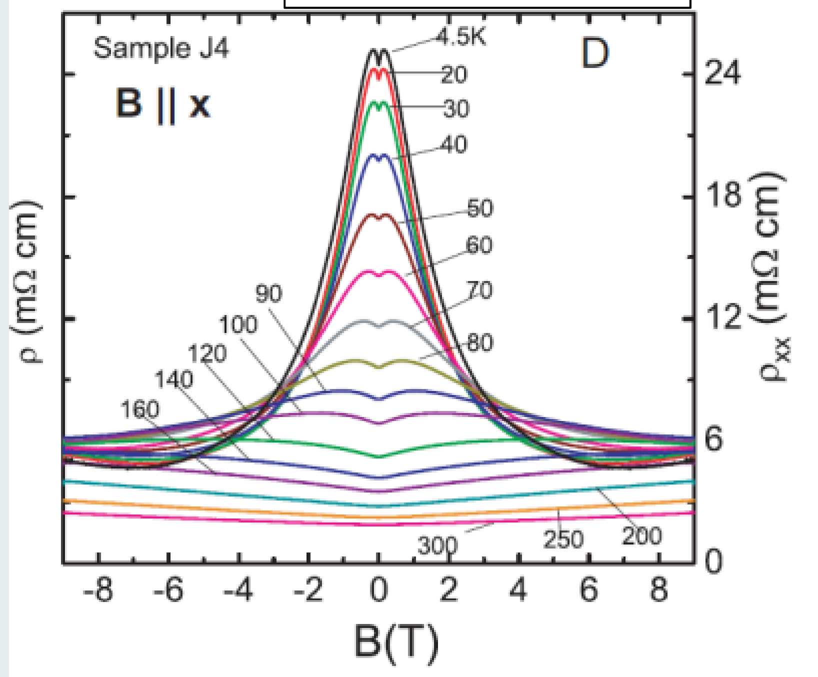

Fermi energy lies 30 meV above node

Striking negative longitud. MR (LMR)

Questions raised by the chiral anomaly expt in Na_3Bi

Experimental Issues

1. Are there other systems, preferably non air-sensitive
2. Dependence on doping (Fermi energy)
3. What about current jetting (spurious effect)?
4. Does chiral anomaly affect other transport quantities
   e.g. thermopower

The chiral anomaly and thermopower of Weyl fermions in the half-Heusler GdPtBi

Max Hirschberger, S. Kushwaha, ZJ Wang, Quinn Gibson, C. Belvin, B. A. Bernevig, R. J. Cava and N. P. O

Nature Materials, online Jun 2016

M. Hirschberger

S. Kushwaha

Zhijun Wang

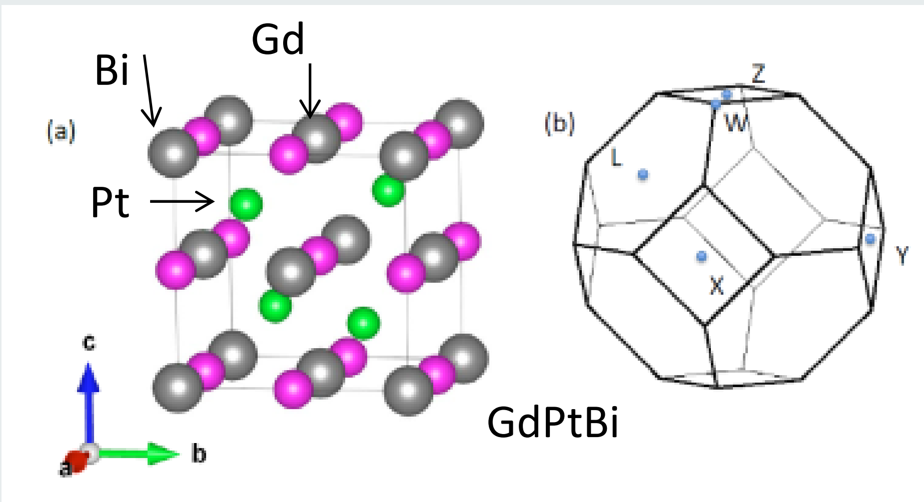

Zinc blende structure (like GaAs)

Except Bi is “stuffed” in fcc sublattice

See also, Checkelsky *Nat. Mat*. 2016

LDA calculations – effect of **B** on bands in GdPtBi

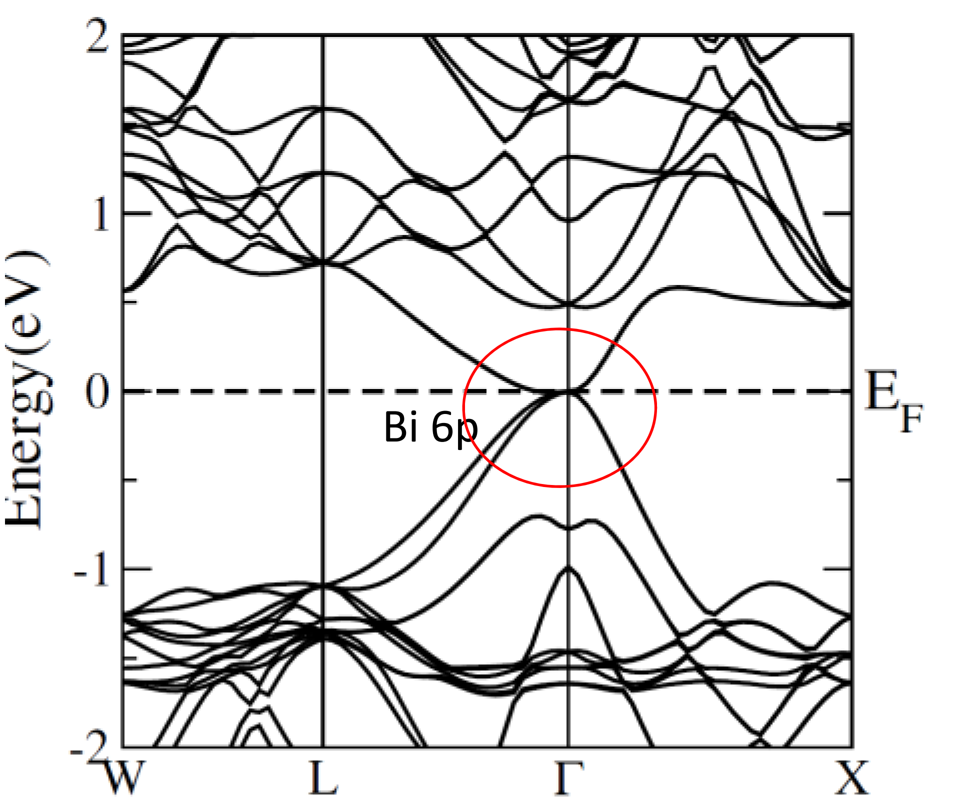

Zhijun Wang

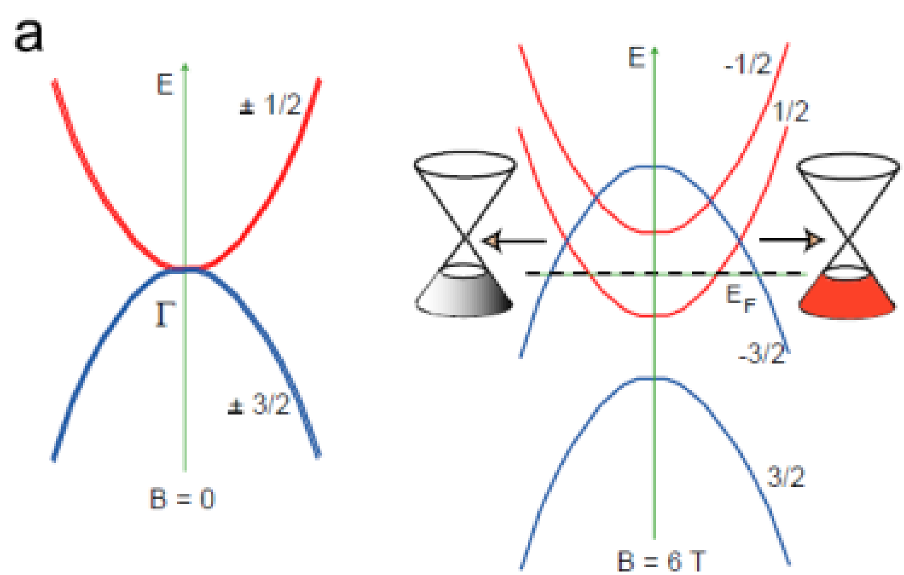

Low-lying states (4) are derived from Bi 6p
Quadratic bands touch at Γ to form zero gap
Large spin orbit coupling

In finite B, large Zeeman field lifts degeneracies
Leads to creation of two Weyl nodes

Weyl nodes created in magnetic field

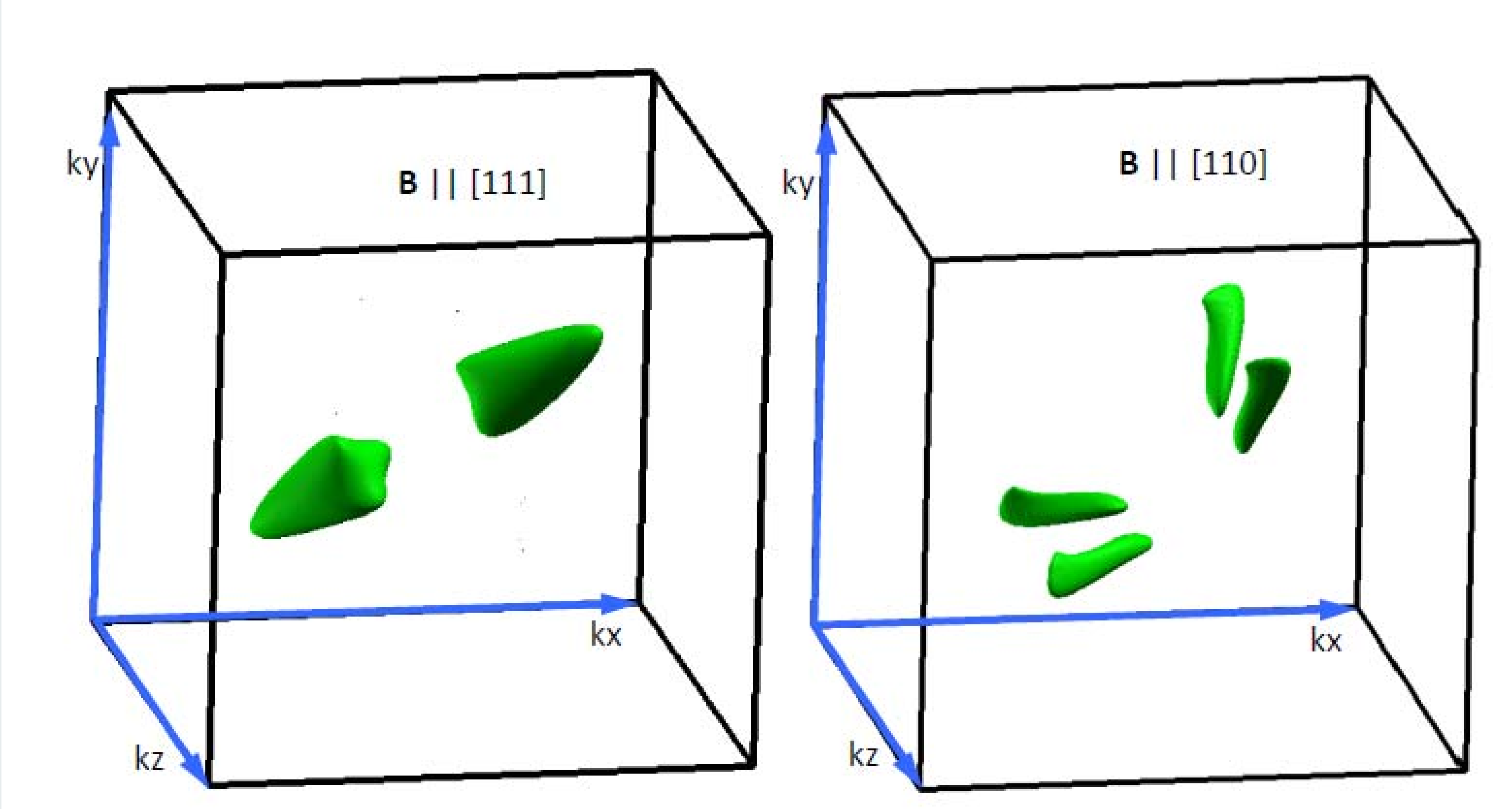

Weyl nodes in a 10-Tesla B (along 111 and 110)
Derived from LDA calculations (Zhijun Wang)

Evidence for chiral anomaly in GdPtBi

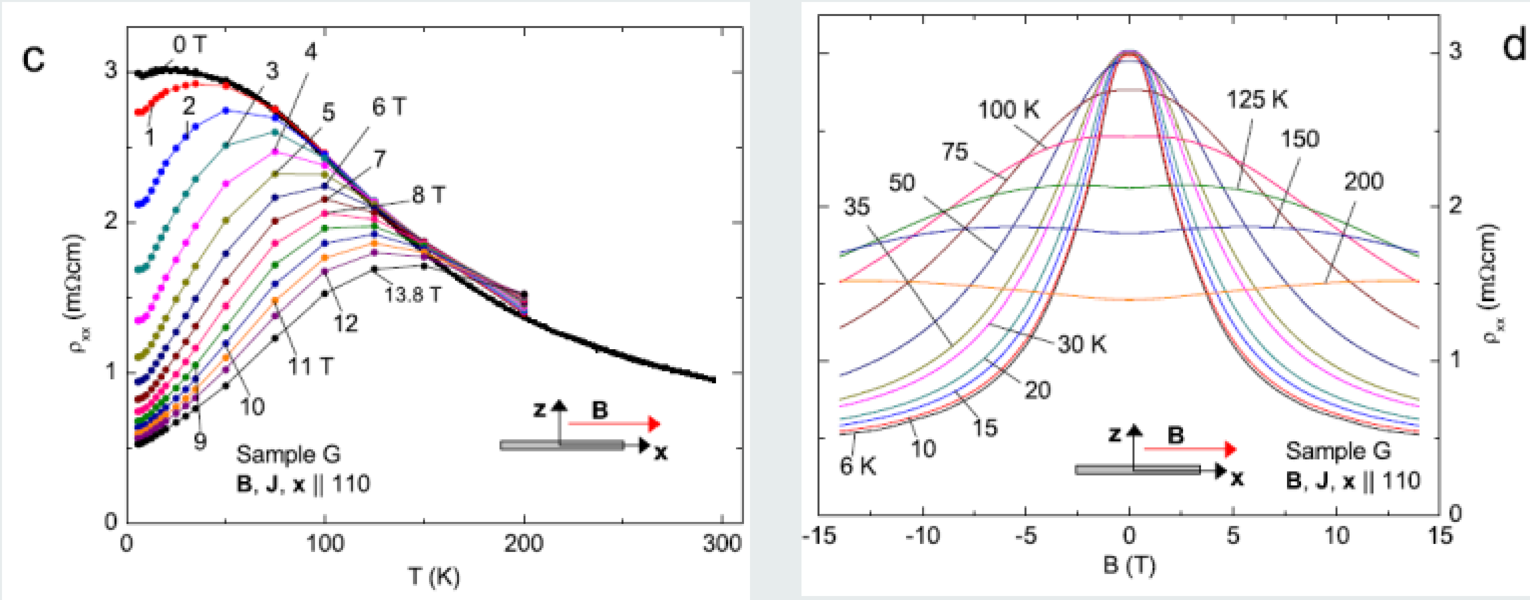

Longitudinal resistivity ρ_{xx} vs. *T* at selected *B*

Large suppression of ρ_{xx} at low *T* and large *B*

MR profile shows large suppression of ρ_{xx} when *B* exceeds ~3 T

Comparison with Na_3Bi suggests existence of chiral anomaly

Resemblance between long. MR in Na_3Bi and GdPtBi

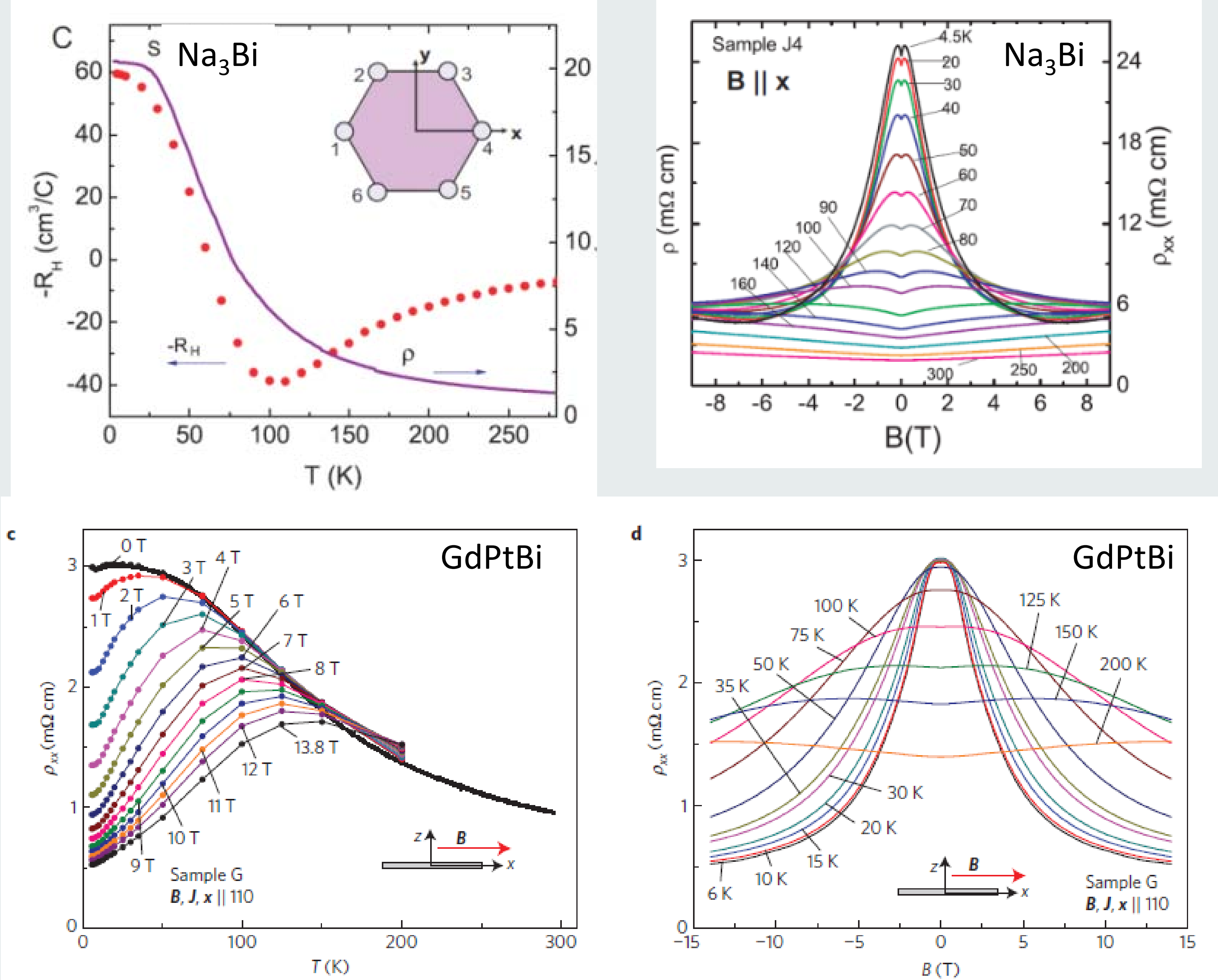

Angular dependence of current plume

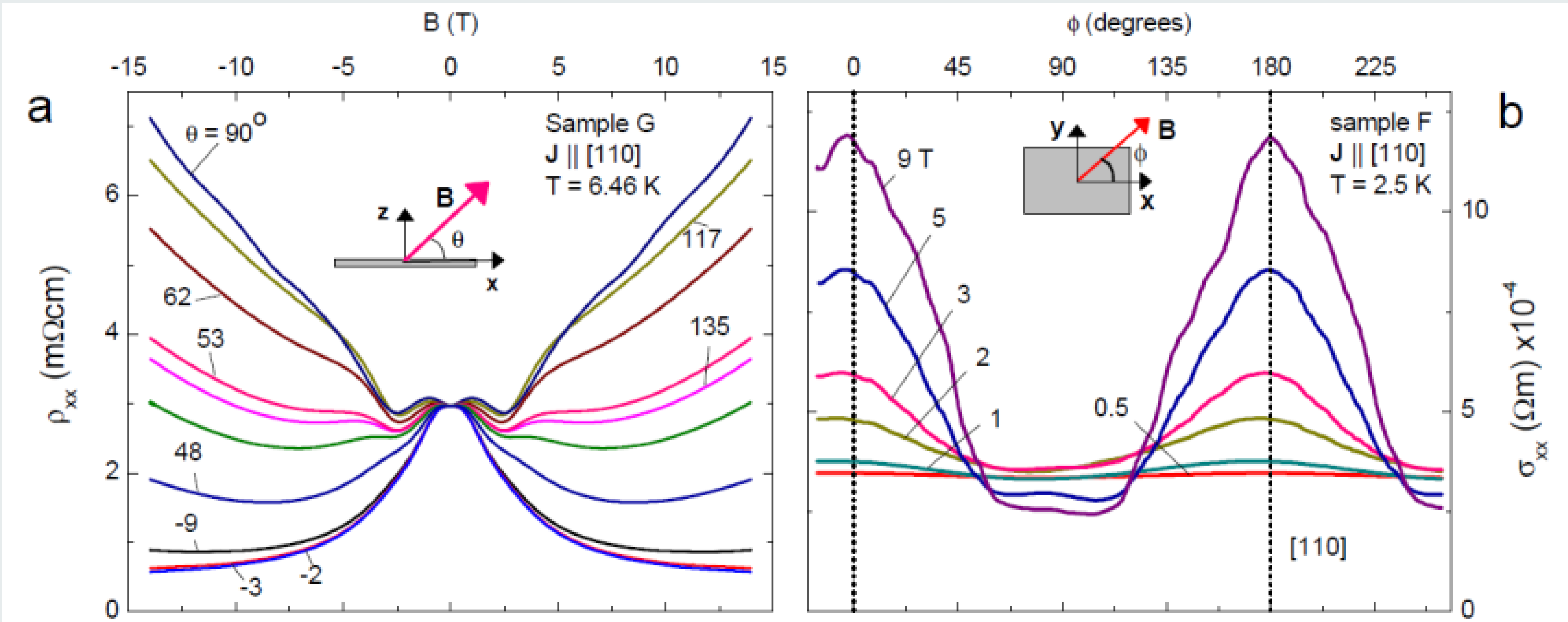

Axial current plume is largest when **B** approaches alignment with **J**

Dependence of resistivity profile on distance of E_F from node

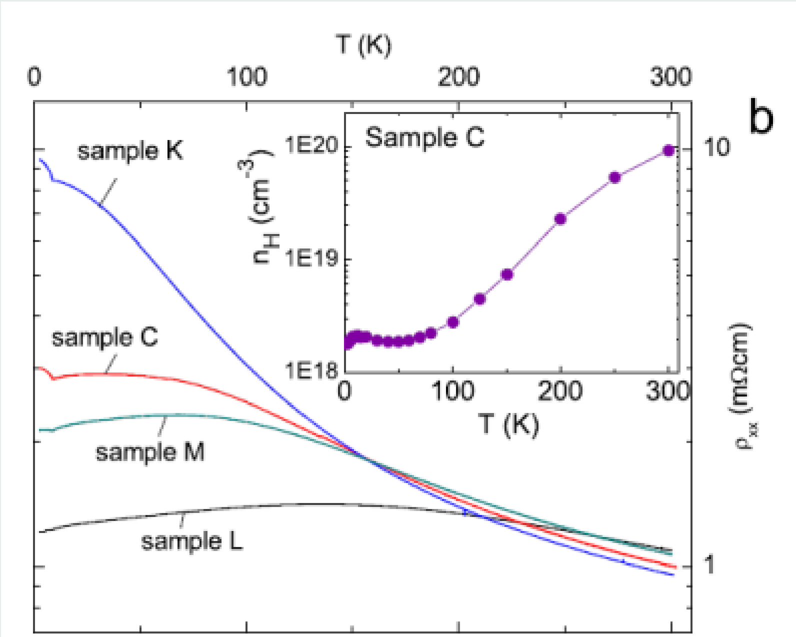

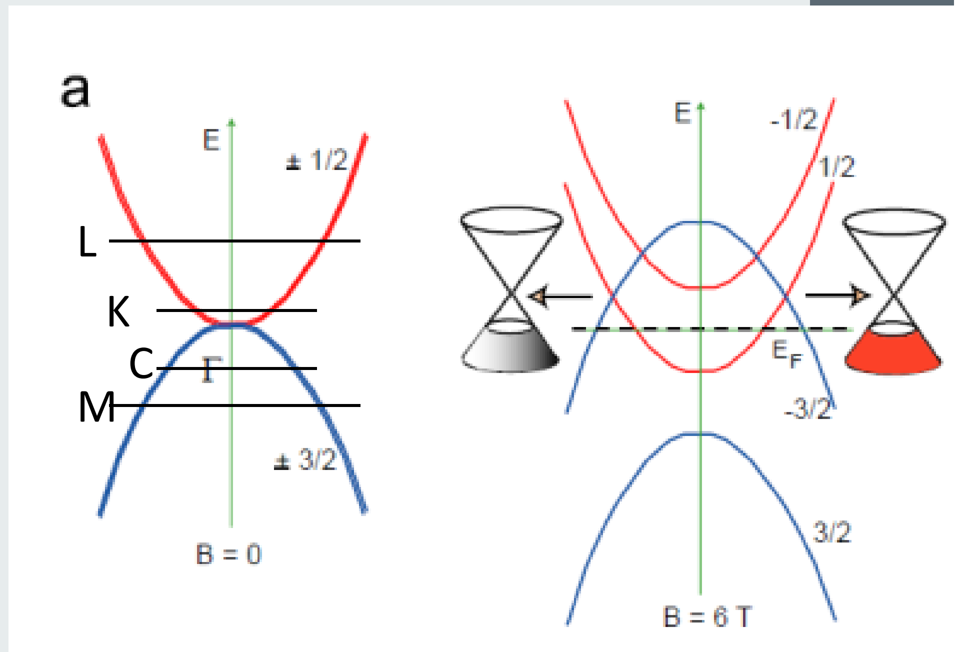

Resistivity profiles are most non-metallic close to node

Dependence of chiral anomaly on distance of E_F from node

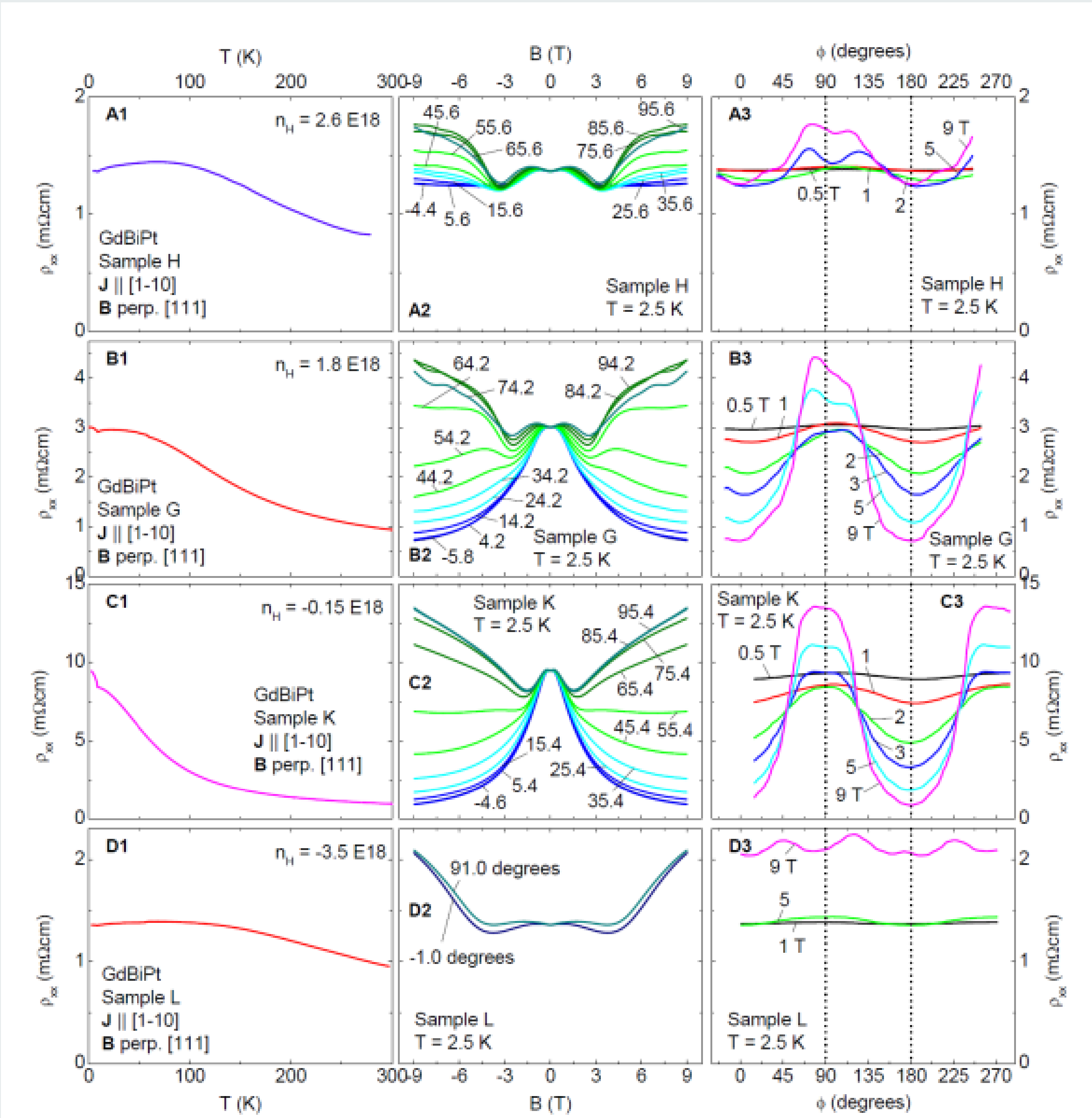

Maximum anomaly ampl. when closest to node

Hole density +2.6 x10^{18}

Hole density +1.8 x10^{18}

Electron density -0.15 x10^{18}

Electron density -3.5x10^{18}

Check for uniformity of current density

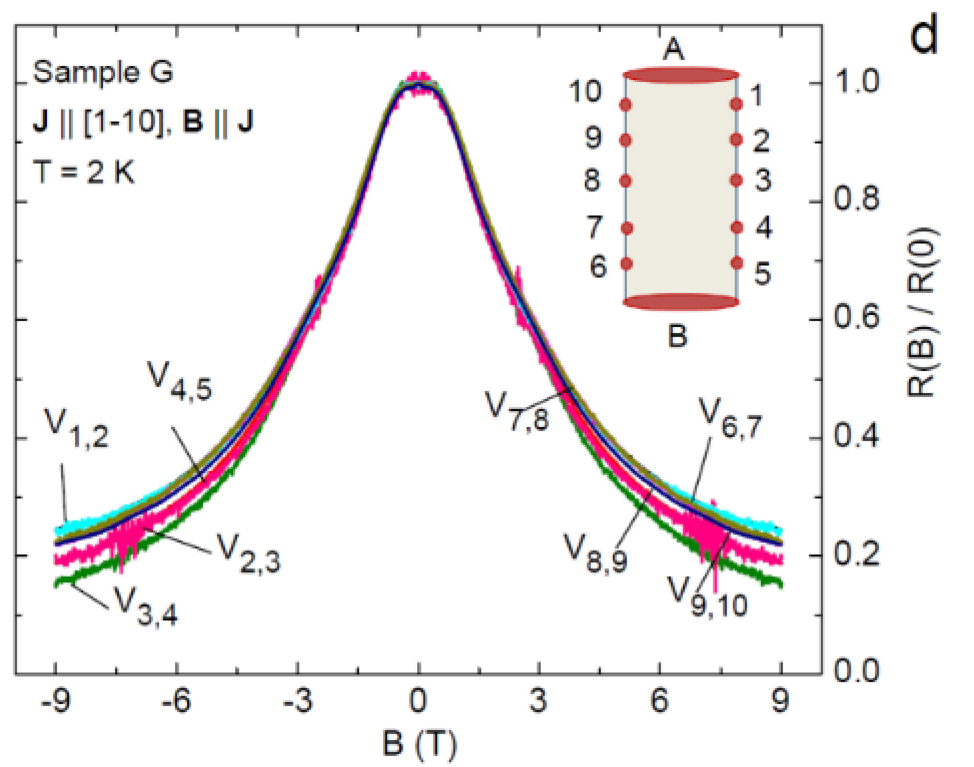

Repeat measmt. on Sample G with 10 voltage contacts
Longitud. MR profiles plotted as relative change are closely similar across all 8 nearest neighbor pairs of contacts

Conclusion: Negative longitude. MR is an intrinsic electronic effect, not a spurious result of inhomogeneity.

“Current jetting”

Current jetting can produce spurious, negative longitud. MR but only in high mobility samples in intense *B* (μB>>1)

$$[\partial_x \sigma_{xx} \partial_x + \partial_y \sigma_{yy} \partial_y]\psi(x,y) = 0.$$

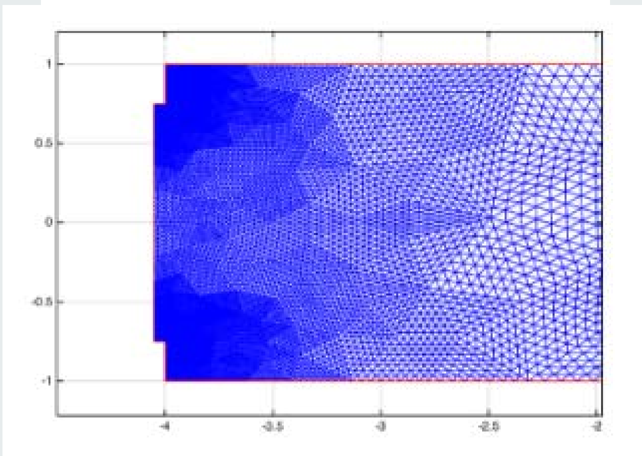

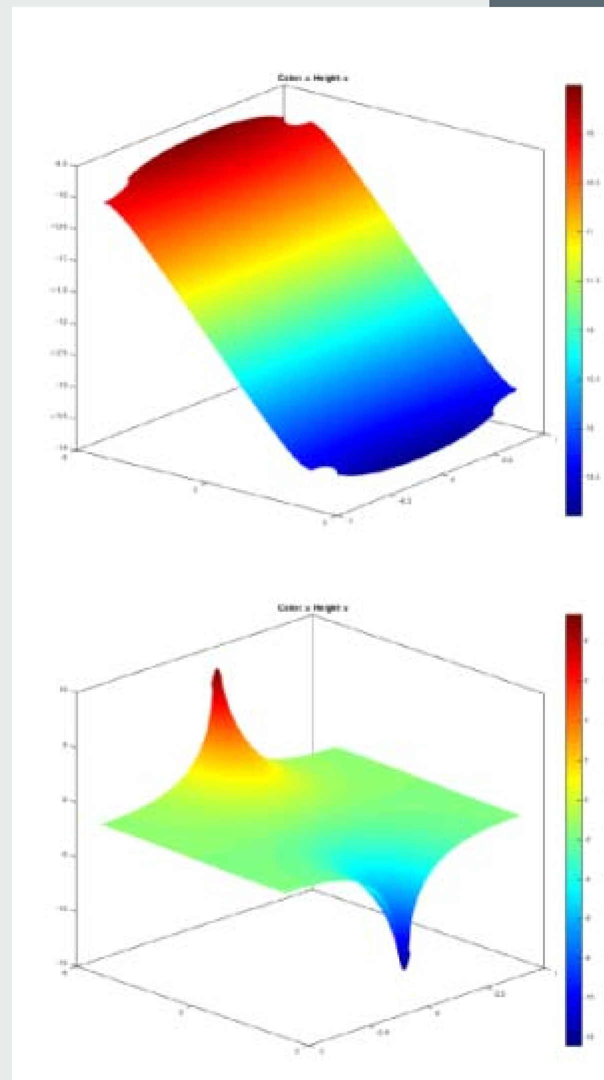

Numerically calculate potential function ψ(x,y) with Drude conductivity tensor in **B** ∥ **E**.
Current jetting is unimportant for small μB and broad current contacts (upper panel). However, for point contacts and large μB (lower panel), get current focusing and jetting (imitates very large contact resistance).

The case against "current jetting" in GdPtBi

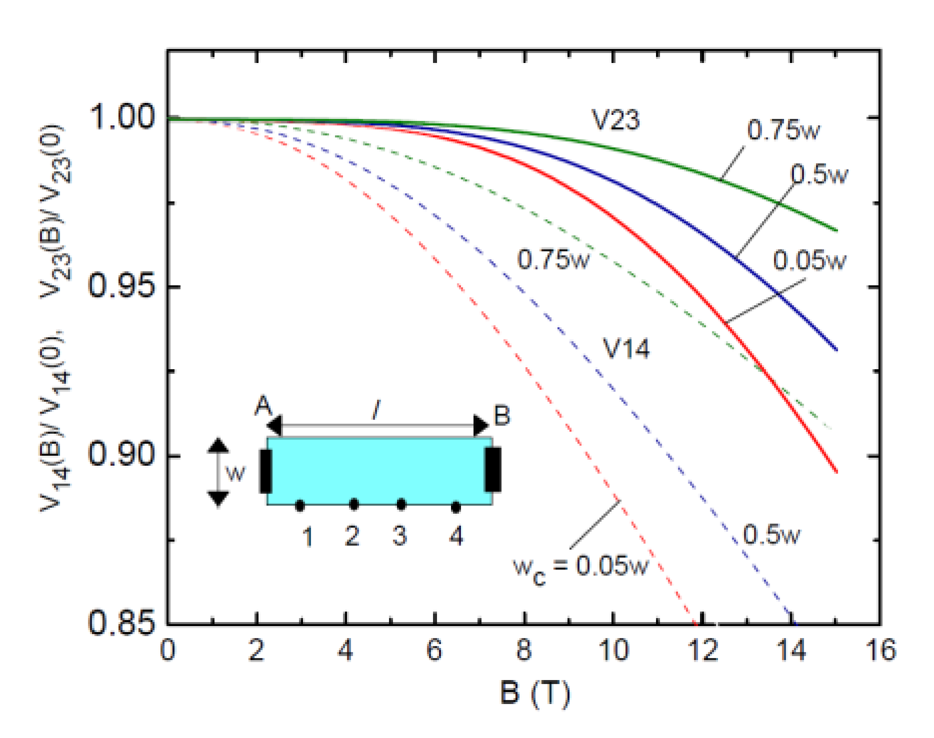

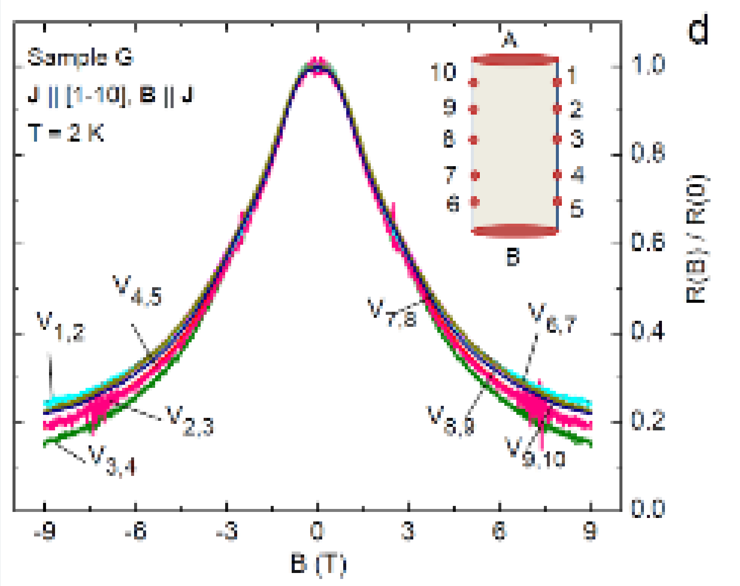

Upper panel:
Calculated $V_{ij}(B)$ curves using "current jetting" assumptions for mobility of 2,000 cm^2/Vs and various current contact widths.

To reproduce observed long. MR curves (lower panel) we would need B to exceed 50 to 70 Tesla.

Conclusion: Current jetting is not the origin of observed chiral anomaly.

Summary of evidence for chiral anomaly in GdPtBi

1. Uniformity of current density **J**(**x**) – an intrinsic effect
2. Narrow plume angle and steerability of plume with **B**
3. Negative longit. MR strongly suppressed when E_F moves away from node
4. Band mass 1.8 (B = 0) much larger than cyclotron mass 0.23 (in finite B)

1. Chiral anomaly in a half Heusler GdPtBi
2. Thermopower of Weyl fermions
3. Gap closing in a semiconductor– route to Weyl nodes
4. Topological metal in PbSnTe with large Berry curvature

Thermopower of Weyl fermions in GdPtBi

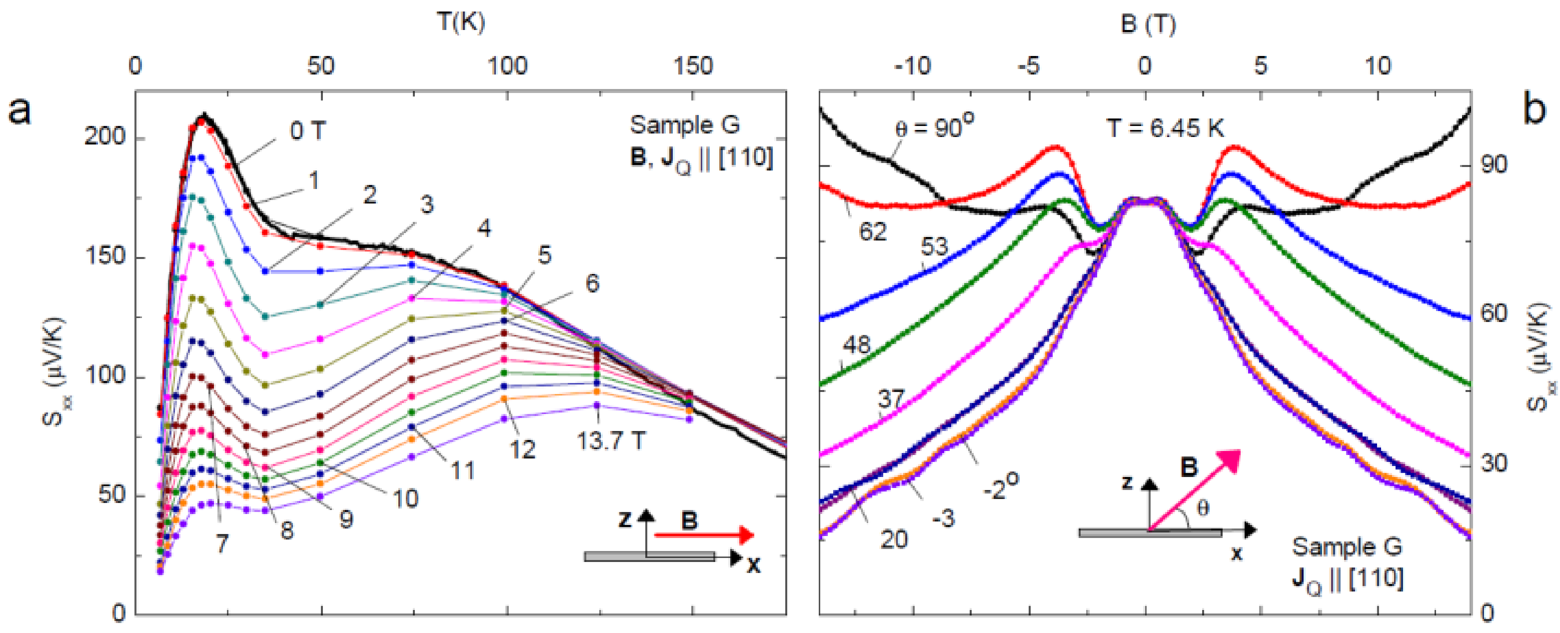

Thermoelectric response is strongly suppressed when axial current appears.

A consequence of chiral n=0 Landau level?

Reflects the “flat” DOS vs. E in the lowest Landau level

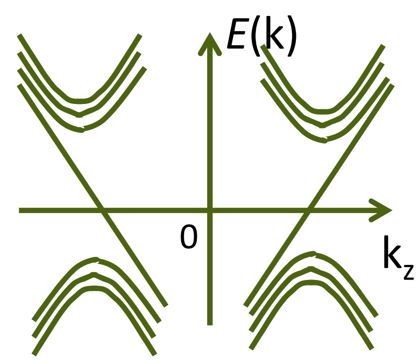

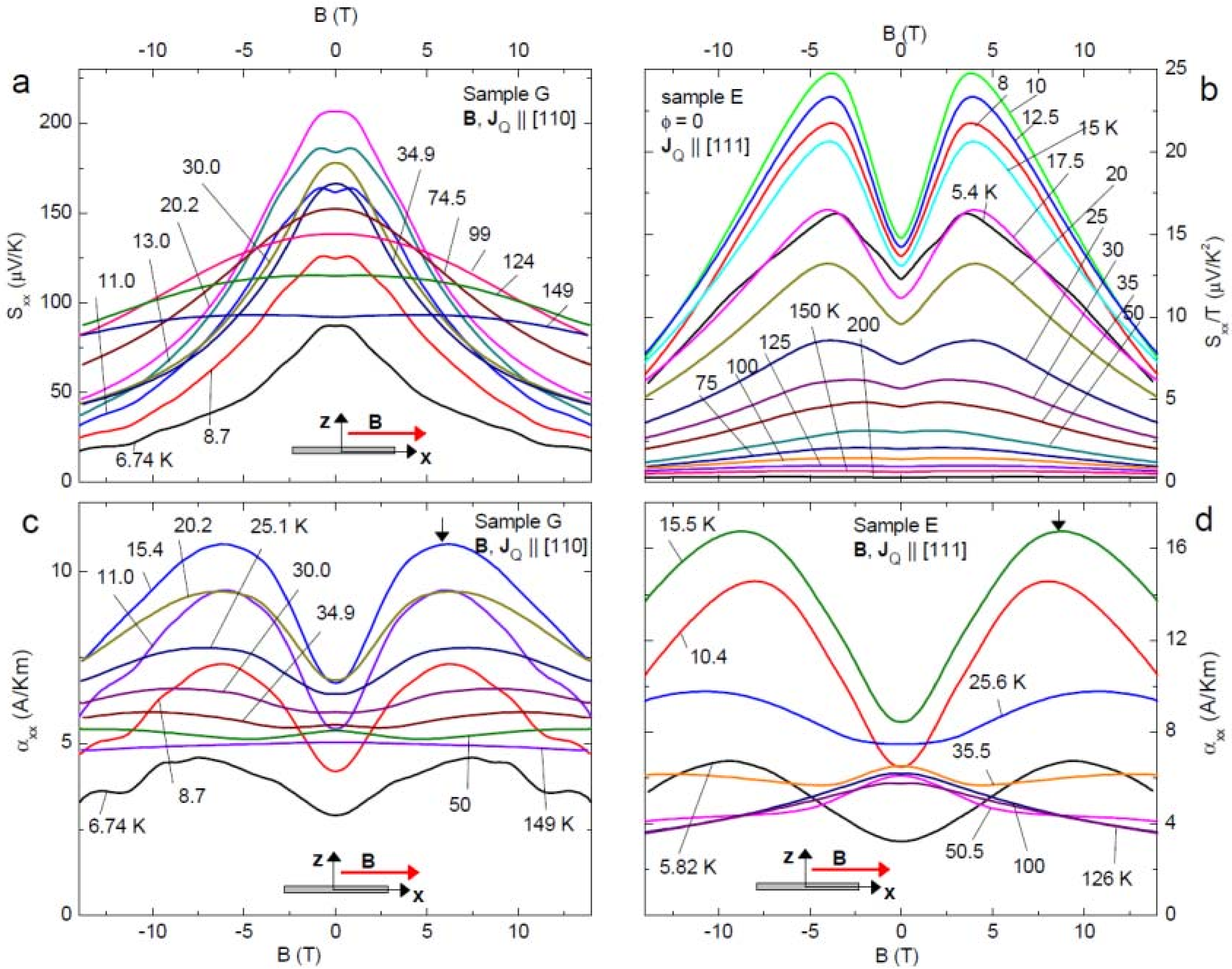

a
Sample G
B, J_Q || [110]
B (T)
S_{xx} (μV/K)
6.74 K
8.7
11.0
13.0
20.2
30.0
34.9
74.5
99
124
149
b
sample E
φ = 0
J_Q || [111]
S_{xx}/T (μV/K^2)
5.4 K
8
10
12.5
15 K
17.5
20
25
30
35
50
75
100
125
150 K
200
c
Sample G
B, J_Q || [110]
α_{xx} (A/Km)
6.74 K
8.7
11.0
15.4
20.2
25.1 K
30.0
34.9
50
149 K
d
Sample E
B, J_Q || [111]
α_{xx} (A/Km)
15.5 K
10.4
25.6 K
35.5
5.82 K
50.5
100
126 K
z
B
x

1. Chiral anomaly in a half Heusler GdPtBi
2. Thermopower of Weyl fermions
3. **Gap closing in a semiconductor– route to Weyl nodes**
4. Topological metal in PbSnTe with large Berry curvature

Royal roads to Weyl Systems

Routes to Weyl fermions

i) Weyl metals TaAs, NbAs, NbP

ii) Dirac semimetals Cd_3As_2, Na_3Bi

iii) Zero-gap semiconductors with strong SOC, GdPtBi, HgCdTe,…

iv) Closing the gap in inversion asymmetric semiconductors (Murakami, 2008)
PbSnTe

v) Single band systems with large Zeeman field $ZrTe_5$, …

Pressure induced topological transition to a metal phase in a narrow gap semiconductor with broken inversion symmetry PbSnTe


Tian Liang

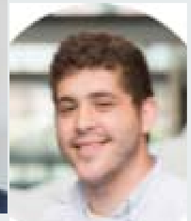
Quinn Gibson


Kushwaha


Jinwoong Kim

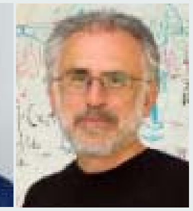
Kioussis

Tian Liang, Satya Kushwaha, Jingjing Lin, Quinn Gibson, Robert Cava, N. P. O.
Princeton University
Jinwoong Kim and Nicholas Kioussis
Cal State Univ. Northridge

What happens when you enforce gap-closing in a semiconductor with broken inversion symmetry?

Evidence for a topological phase transition.
Provides a new route to Weyl fermions

Universal phase diagram in 3D

S. Murakami

SM, New J. Phys. ('07).
SM. Kuga, PRB ('08)
SM, Physica E43, 748 ('11)

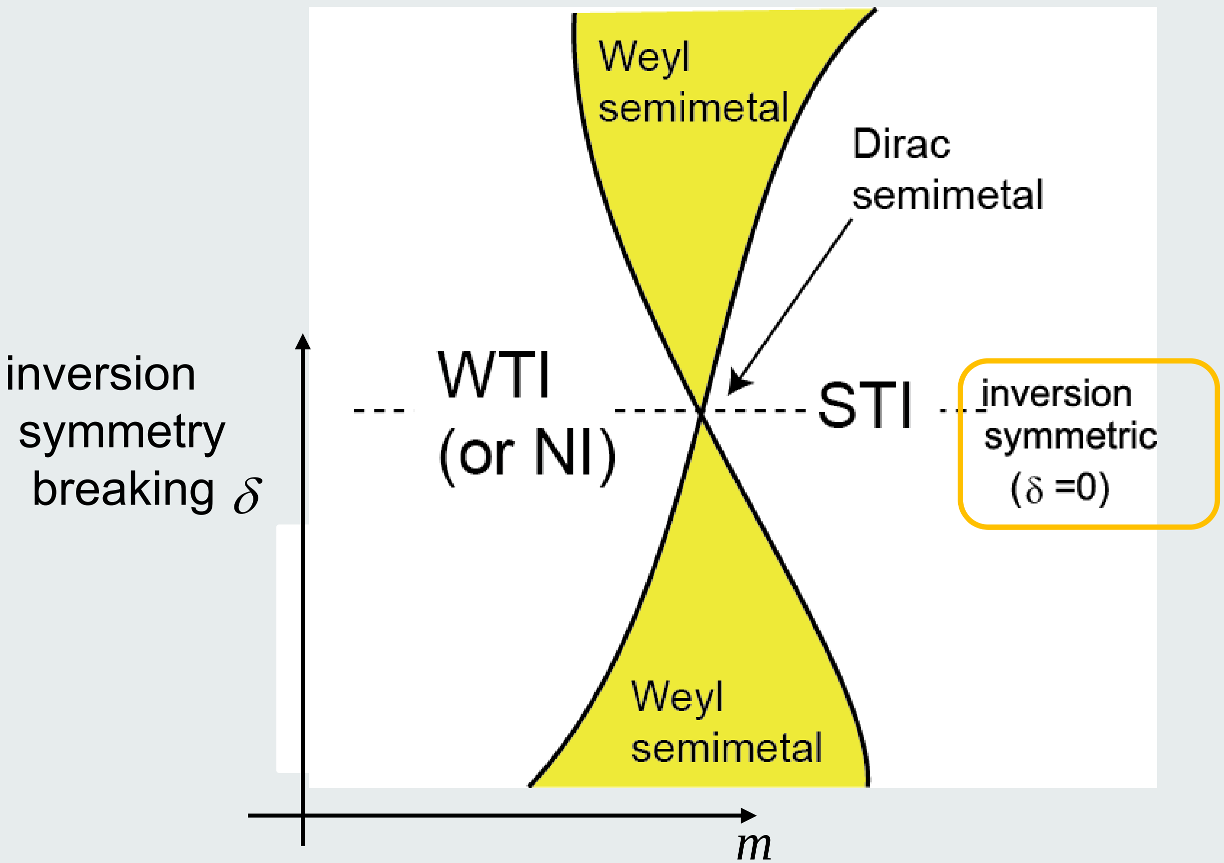

external parameter
(e.g.: pressure, atomic composition, SOC etc.)

Closing the gap in a 3D semi-conductor

Closing the gap in a semiconductor by pressure, doping etc

Murakami, New J. Phys. (‘07).
Murakami. Kuga, PRB (’08)
Murakami, Physica E(‘11)
Okugawa, Murakami, PRB(’14)

⟶ m

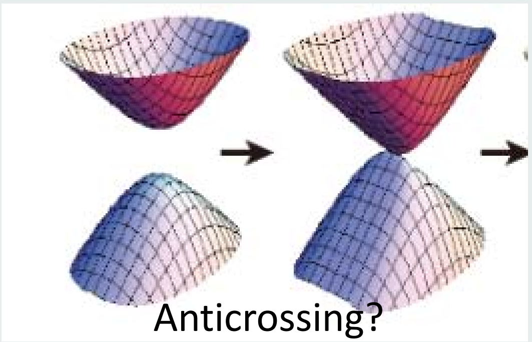

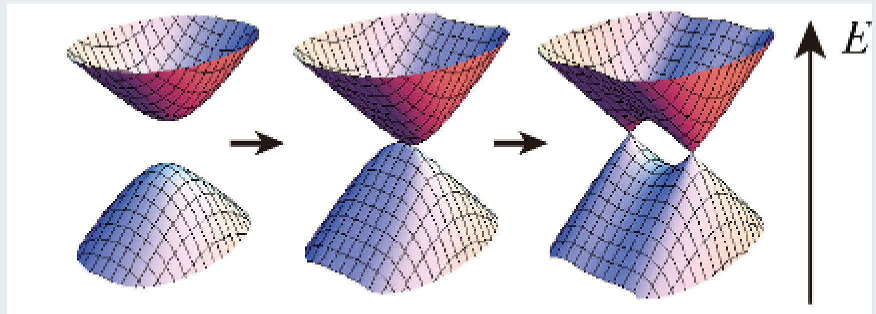

Discrete point nodes

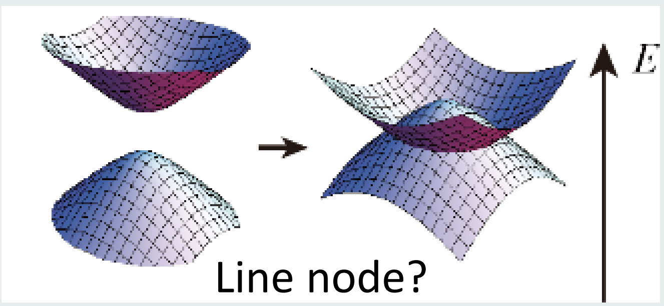

Weyl nodes

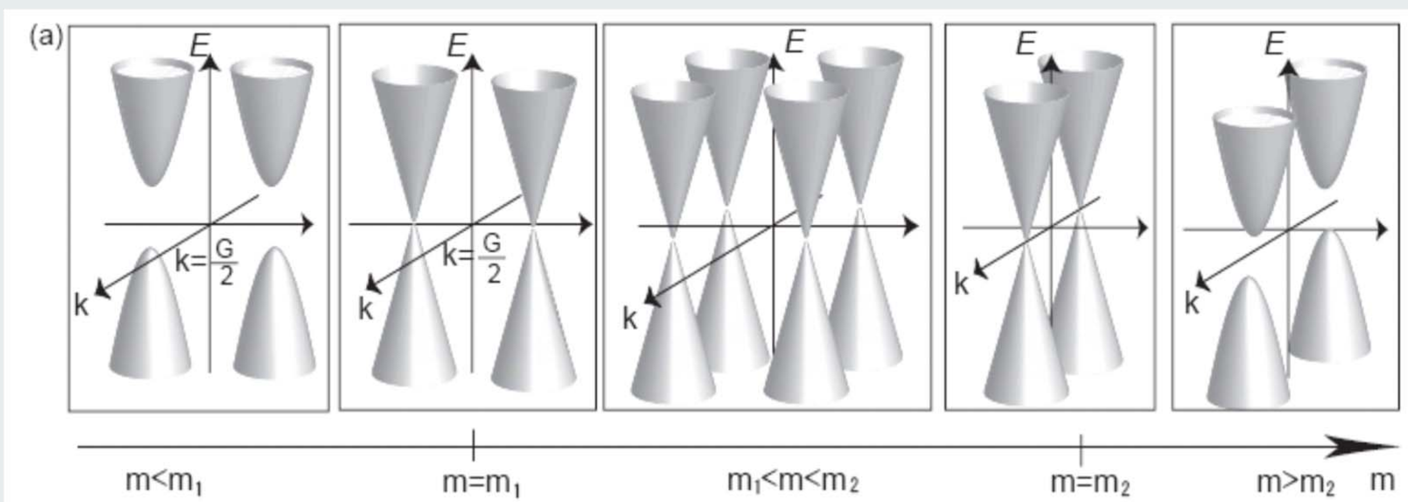

Rocksalt PbSnTe – narrow gap semiconductor lacking inversion symmetry

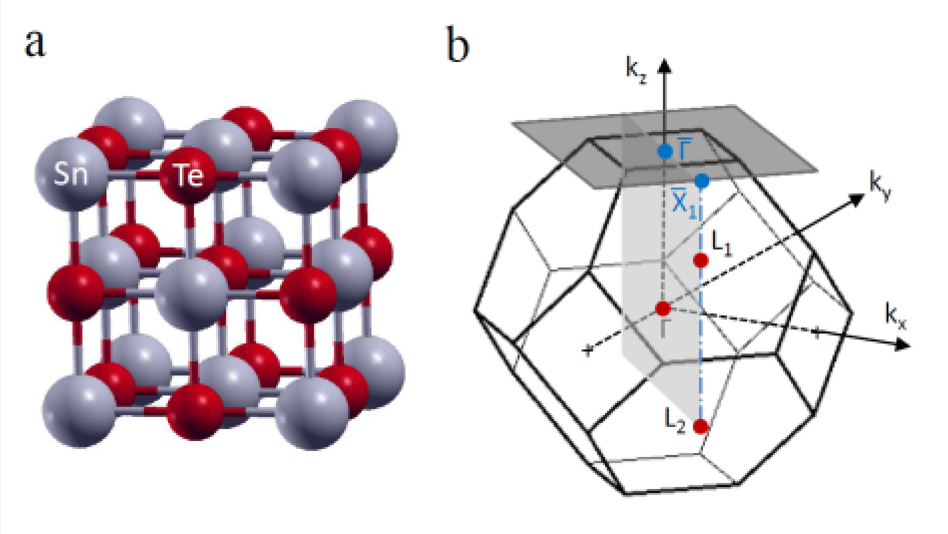

Rocksalt structure (like NaCl)

Inversion symmetry broken by slight compression along [111] (body diagonal)

Recent renewed interest as topological crystalline insulator
Here, we focus on the bulk states --- massive Dirac states at L points (center of hexagons in BZ)

Investigate two compositions; x(Sn) = 0.5 and x(Sn) = 0.25

Pressure induces insulator-metal-insulator transitions

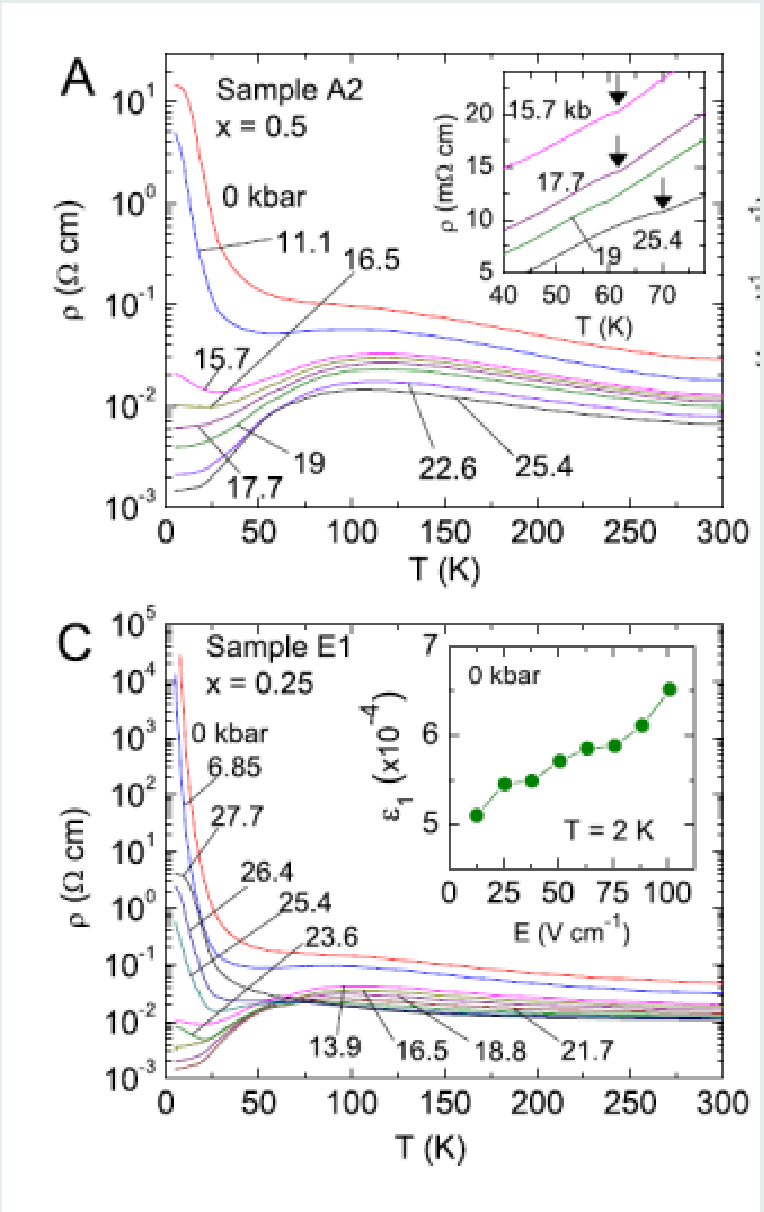

Tian Liang

Upper inset:

A weak feature in resistivity signals transition to inversion broken state (arrows)

Lower inset:

Dielectric measurements yield a very large dielectric coefficient

$\varepsilon_1 \sim 5 \times 10^4$

with spontaneous polarization (when $E \rightarrow 0$)

(Main panel upper)

Under pressure

Sample A2 (x = 0.5) becomes metallic at 15 kbar

(Lower panel)

Sample E1 (x = 0.25), becomes metallic at 12 kbar; returns to insulator at 25 kbar. Resistivity falls by 7 orders.

Phase diagram of insulator-metal-insulator transitions

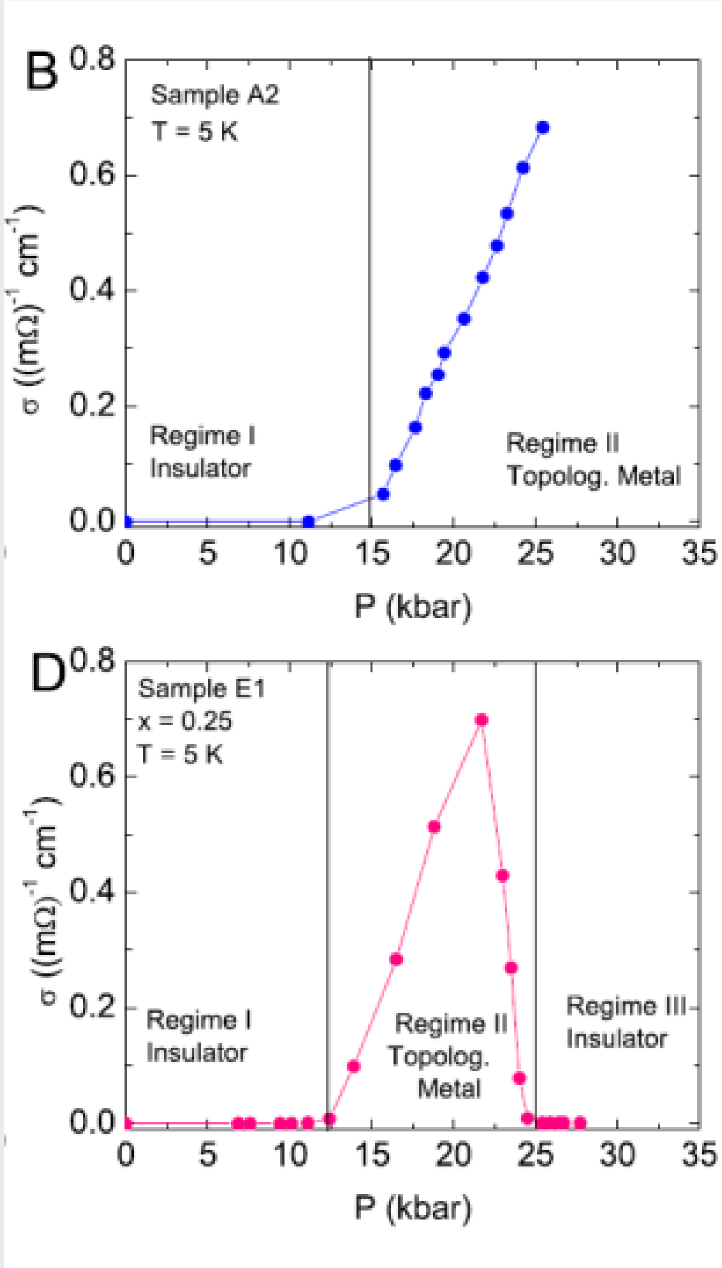

(Upper panel)
Sample A2 ($x = 0.5$)
IM transition at P1 = 15 kbar

(Lower panel)
Sample E1 ($x = 0.25$)
IM transitions at P1 = 12.5 kbar
MI transition at P2 = 25 kbar

LDA calculations confirm Murakami's scenario for Weyl creation

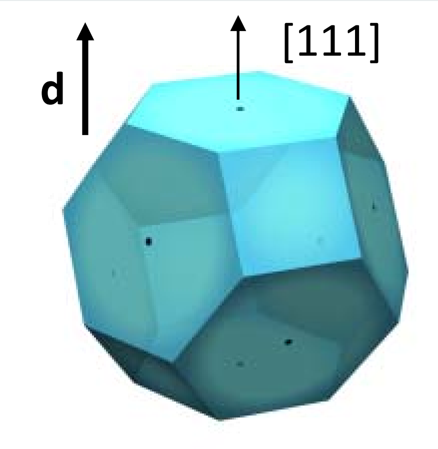

Brilloiun Zone
with assumed
distortion [111]

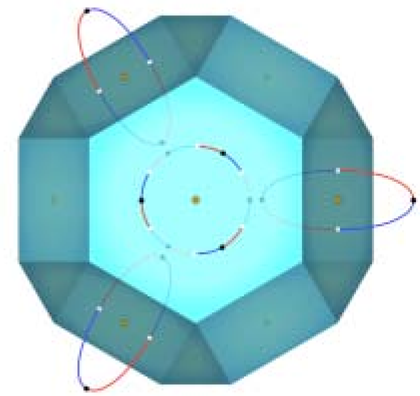

Trajectories of Weyl nodes
Vs pressure (view along [111])

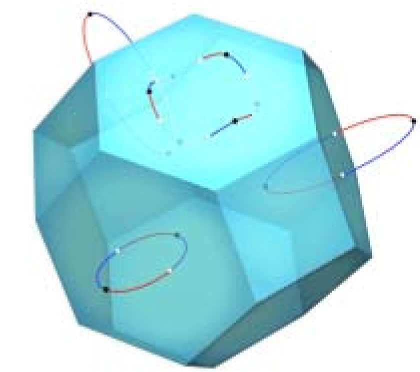

Trajectories
(tilted view)

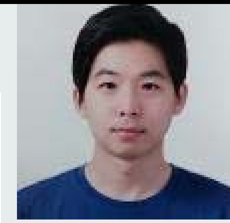

Jinwoong Kim

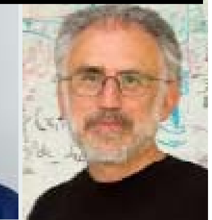

Kioussis

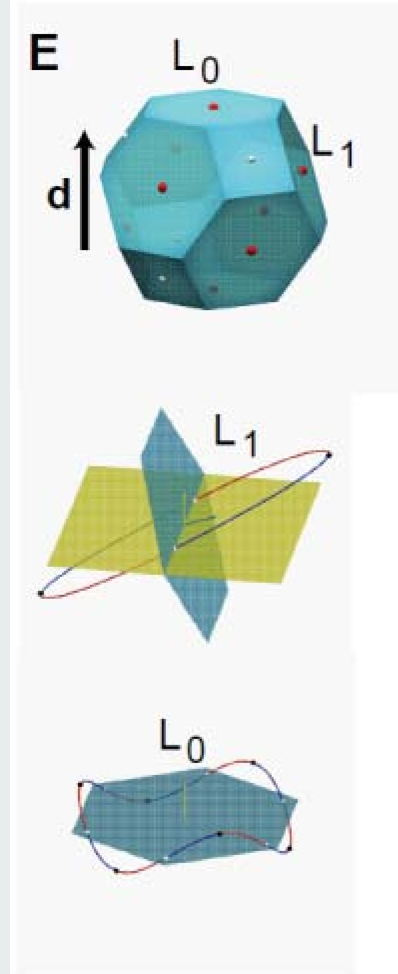

Pressure spawns small FS seen by quantum oscillations

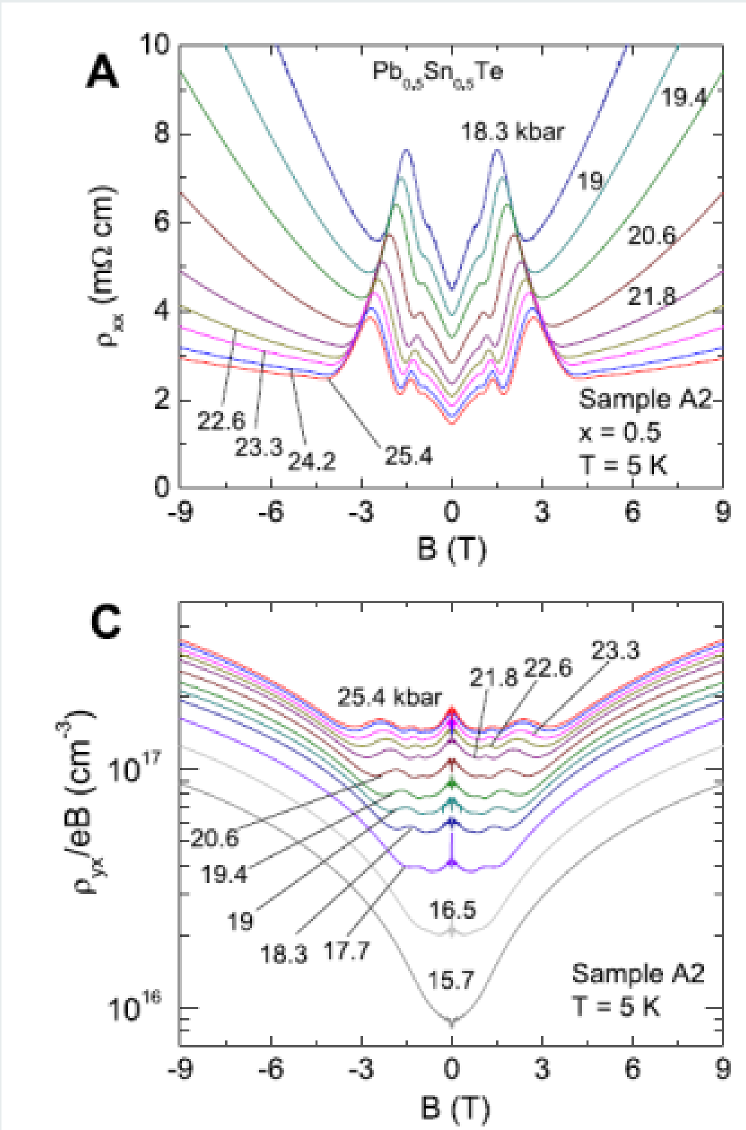

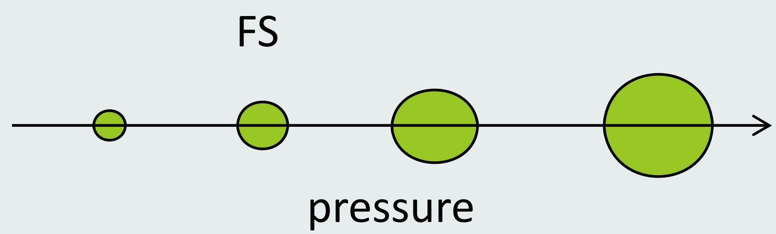

(Upper panel) Transverse MR in Sample A2 FS caliper S_F from SdH oscillations grows with pressure.

(Lower panel) Hall resistivity ρ_{yx} divided by field vs B. Flat portion at low B directly measures the Hall density $n_H = \rho_{yx}/eB$

At large B, ρ_{yx} deviates strongly from Drude response (note log scale)

1. Chiral anomaly in a half Heusler GdPtBi
2. Thermopower of Weyl fermions
3. Gap closing in a semiconductor– route to Weyl nodes
4. **Topological metal in PbSnTe with large Berry curvature**

Berry Curvature and the anomalous Hall effect

Luttinger

Karplus Luttinger theory (1954) anticipated Berry curvature

$\mathbf{A}(\mathbf{k}) = (u_{\mathbf{k}}, i\nabla u_{\mathbf{k}})$ (Berry vector potential)

$\mathbf{\Omega}(\mathrm{k}) = \nabla\times \mathbf{A}(\mathbf{k})$

$\mathbf{v}(\mathbf{k}) = \nabla_{\mathbf{k}}\varepsilon + \mathbf{E}\times\mathbf{\Omega}(\mathbf{k})$ Luttinger anomalous velocity $\mathbf{v}_{\mathrm{A}}$

$$\mathbf{J} = 2\boldsymbol{e}\sum_{\mathbf{k}} \boldsymbol{f}_{\mathbf{k}}^{0}\,\mathbf{v}_{\mathbf{k}} + \boldsymbol{e}^{2}\mathbf{v}\times\mathbf{B}\cdot\left(-\frac{\partial \boldsymbol{g}(\mathbf{k})}{\partial\mathbf{k}}\right)\mathbf{v}\,\tau$$

Anomalous velocity makes first term finite.
Prop. to f^0 and E, but *independent* of B apart from direction (spontaneous).
Independent of τ.
Engendered 50 years of tortured, confused debate.
Now accepted as intrinsic cause of AHE.

Breaking of TRS; Appearance of Berry curvature

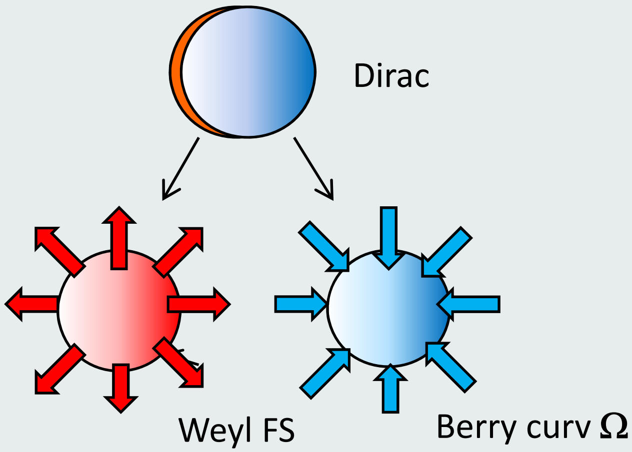

Each Weyl node is a monopole source of Berry flux

$$\chi = \frac{1}{2\pi}\oint \boldsymbol{\Omega}\cdot \mathbf{dS}(\mathbf{k})$$

with Berry curvature given by

$$\boldsymbol{\Omega}(\mathbf{k}) = \nabla \times \mathbf{A}(\mathbf{k}) \qquad \mathbf{A} = i(u_{\mathbf{k}}, \nabla u_{\mathbf{k}})$$

$\boldsymbol{\Omega}(\mathbf{k})$ produces an anomalous velocity that modifies eqns of motion

$$\dot{\mathbf{r}} = \nabla_{\mathbf{k}}\, \boldsymbol{\varepsilon}(\mathbf{k}) - \dot{\mathbf{k}} \times \boldsymbol{\Omega}(\mathbf{k})$$
$$\dot{\mathbf{k}} = \boldsymbol{e}\mathbf{E} + \boldsymbol{e}\,\dot{\mathbf{r}} \times \mathbf{B}$$

Berry curvature adds an anomalous Hall current to conventional Hall.
However, we need to break TRS

In PbSnTe, TRS is broken by large Zeeman field

Anomalous contribution to Hall effect

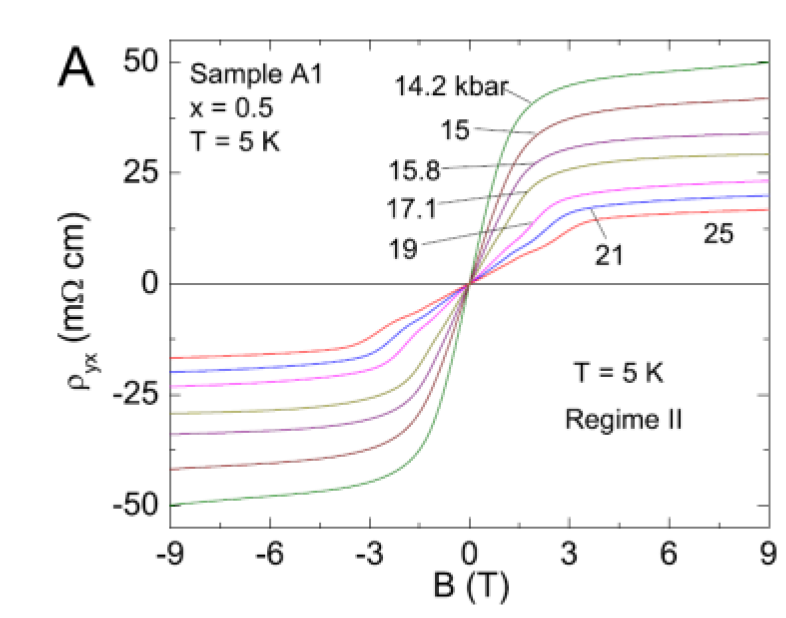

(Upper panel) The observed Hall resistivity ρ_{yx} in topol metal phase. Flattening of ρ_{yx} at large *B* from a large anomalous contrib

$\sigma_{xy} = \sigma_{xy}{}^{N} + \sigma_{xy}{}^{A}$

(Otherwise ρ_{yx} should be linear in *B*).

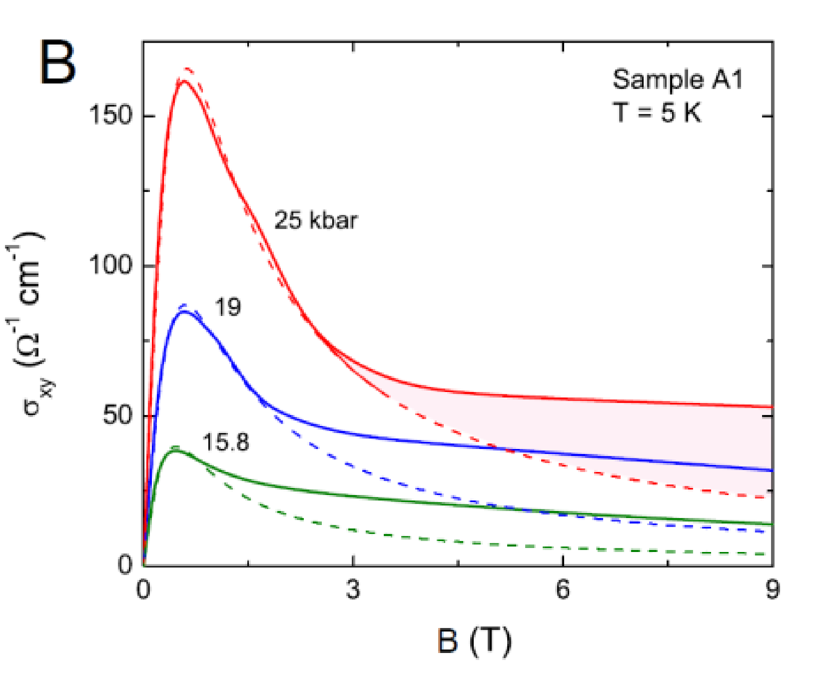

(Lower panel)
Plot of σ_{xy} vs *B* at 3 pressures. Dashed curves are fits to Drude response.
Mobility μ_e = ~40,000 cm^2/Vs
Excess Hall current (shaded) is the anomalous term $\sigma_{xy}{}^{A}$ that is *induced* by **B**

Contrast with AHE in ferromagnet

Weyl nodes shifted asymmetrically in energy by Zeeman field

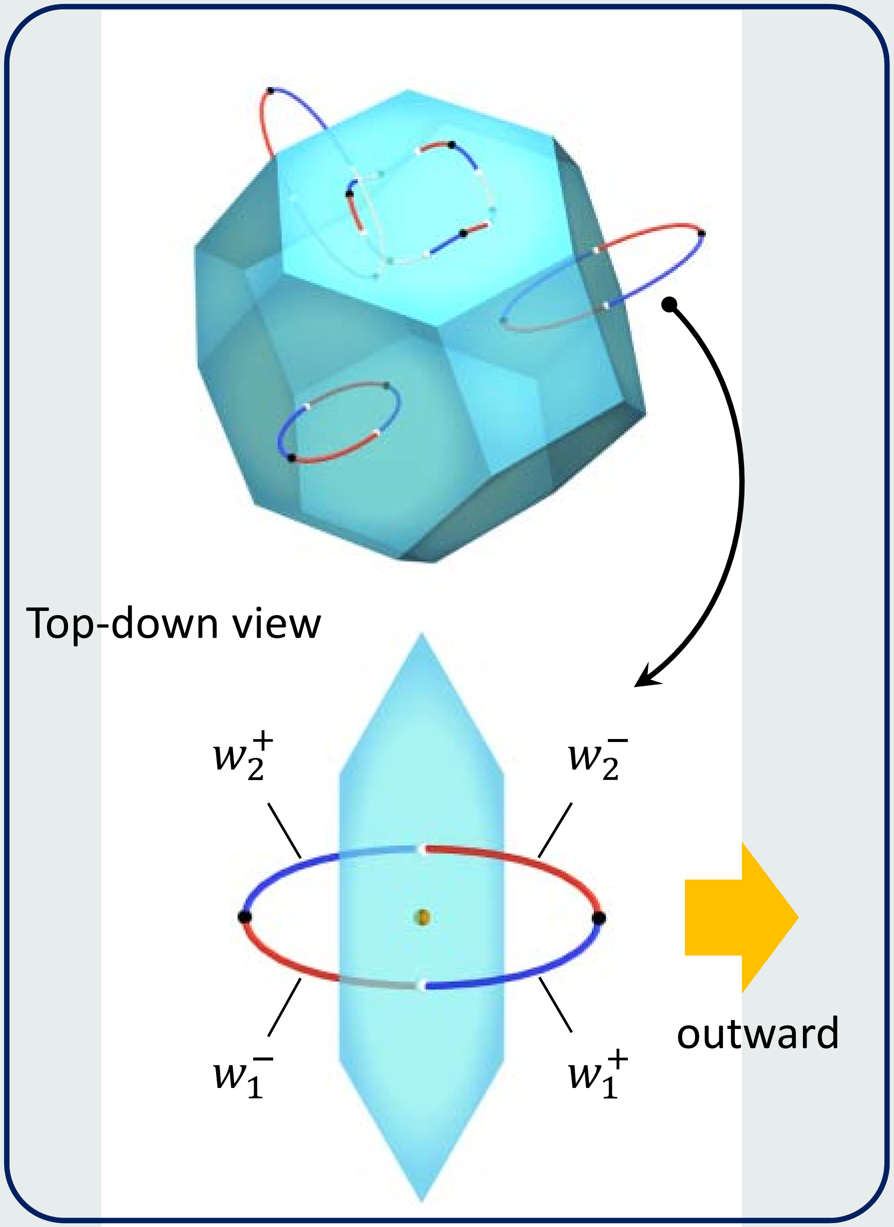

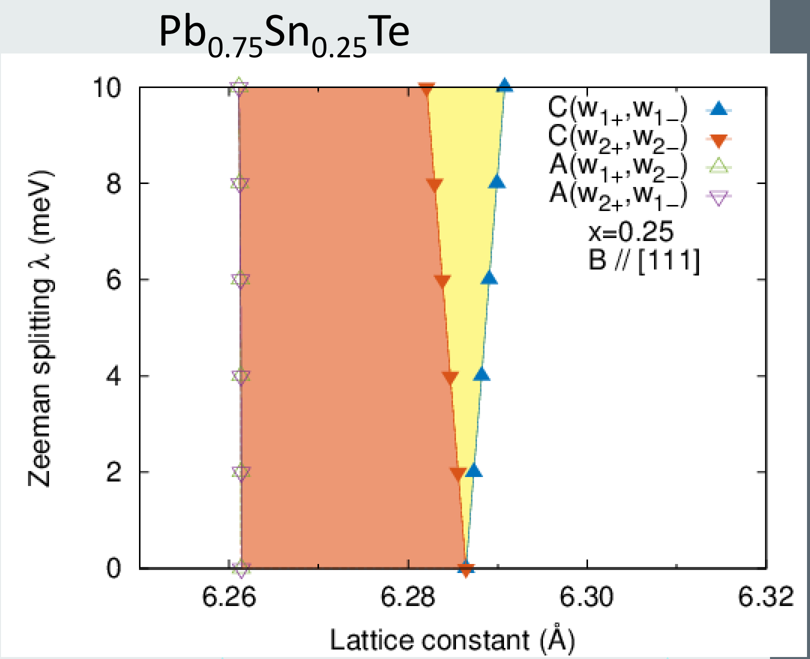

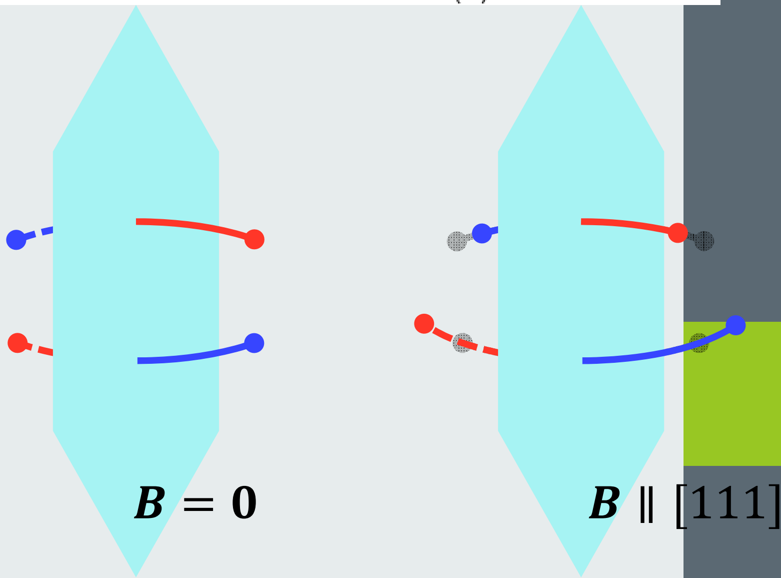

Summary

Closing of energy gap by pressure is nontrivial when inversion symm is broken.
Weyl nodes are pair created in metallic phase (Murakami et al.)

Annihilation of Weyl nodes recovers insulating gap.

Strong evidence that PbSnTe illustrates this scenario.

1. Inversion symmetry is broken

2. Under pressure, we find a metallic phase sandwiched btw insulating states.

3. Metallic phase has 12 identical FS pockets

4. Hall response reveals large Berry curvature induced by applied field

5. LDA calculations confirm Weyl node formation and asymmetry in Zeeman field

Summary

1) Evidence for chiral anomaly in Dirac semimetal Na_3Bi

2) Chiral anomaly in a zero-gap semiconductor, half Heusler GdPtBi
   Zeeman field induces band crossing and protected nodes
   Chiral anomaly has strong effect on thermoelectric current

3) Observation of negative, longitudinal MR in $ZrTe_5$
   Find large, in-plane anomalous Hall effect

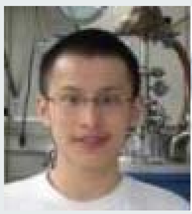
Jun Xiong


Kushwaha


Tian Liang


Jason Krizan


Hirschberger


Zhijun Wang

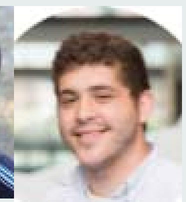
Quinn Gibson


Cano


Bradlyn


Jinwoong Kim

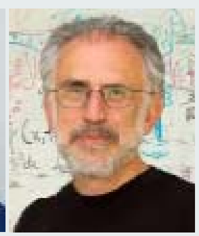
Kioussis


Bob Cava


Bernevig


NPO

Thank you